An indoor positioning system for mobile target tracking based on VLC and IMU fusion

Zou Qian   Xia Weiwei   Zhang Jing   Huang Bonan   Yan Feng   Shen Lianfeng

(National Mobile Communications Research Laboratory, Southeast University, Nanjing 210096, China)

Abstract: An indoor positioning system (IPS) is designed to realize positioning and tracking of mobile targets, by taking advantages of both the visible light communication (VLC) and inertial measurement unit (IMU). The platform of the IPS is designed, which consists of the light-emitting diode (LED) based transmitter, the receiver and the positioning server. To reduce the impact caused by measurement errors, both inertial sensing data and the received signal strength (RSS) from the VLC are calibrated. Then, a practical propagation model is established to obtain the distance between the transmitter and the receiver from the RSS measurements. Furthermore, a hybrid positioning algorithm is proposed by using the adaptive Kalman filter (AKF) and the weighted least squares (WLS) trilateration to estimate the positions of the mobile targets. Experimental results show that the developed IPS using the proposed hybrid positioning algorithm can extend the localization area of VLC, mitigate the IMU drifts and improve the positioning accuracy of mobile targets.

Key words: indoor positioning system (IPS); visible light communication (VLC); inertial measurement unit (IMU); hybrid positioning algorithm

Ⅰ n recent years, the applications of wireless sensor networks are becoming increasingly essential in our daily life. Location information becomes important in location-based services (LBS) with the popularization of mobile communication and the Internet[1]. The global positioning system (GPS) cannot support indoor positioning due to the blocking of electromagnetic signals and multipath interference. Numerous research and solutions for GPS complementation have emerged in the past decades. Among the radio indoor positioning systems, the system based on visible light communication (VLC) is more accurate than those based on wireless local area networks (WLAN) and radiofrequency identification (RFID),

more stable than that based on Bluetooth (BT), and cheaper than that based on ultra-wide band (UWB) [2].

Optical wireless communication has gained much attention, which transmits the data through air using infrared (IR) and VLC[3-4]. Positioning based on VLC is preferred due to no electromagnetism, long lifespan, low cost and no health risks. VLC with a light-emitting diode (LED) has a shorter wave than the radio frequency in reducing multipath effects in an indoor environment. The positioning techniques used in location estimation are based on the geometric properties of triangles including triangulation and trilateration[5]. Since VLC is limited by the field of view, the triangulation method based on the angle of arrival (AOA) is not suitable. The trilateration method based on time of arrival (TOA) or time difference of arrival (TDOA) requires that the transmitter and receiver keep strict synchronization. Therefore, these methods are not applicable for VLC positioning. In this paper, the method based on received signal strength (RSS) is used since it is easy to achieve and can provide better accuracy.

Measurement from the inertial measurement unit (IMU) accounts for the relative estimation of position with low cost and reasonable accuracy. IMU consists of accelerometers, gyroscopes and electronic compasses and it can measure the acceleration and angular velocity[6]. However, IMU has long term drift and is sensitive to initialization of positioning. Hence, it is necessary to enhance the positioning accuracy with calibration and it also needs to be used with the integration of other measurements[7].

There is some research on realizing indoor positioning based on VLC[8-10], which communicates via wired connection in a limited positioning range. As for the IMU positioning system, due to its error-accumulation, it is not reliable enough for indoor positioning independently[11-12]. The indoor environment has many barriers for VLC positioning and the IMU cannot reduce the drifts by itself. To solve the practical problem and take advantages of VLC and IMU, an indoor positioning system (IPS) based on VLC and IMU is developed to extend the localization area of VLC and reduce IMU drifts.

In this paper, an IPS is developed by using the hybrid positioning algorithm, which consists of the LED transmitter, receiver and localization server. Before positioning, the calibration and normalization of VLC RSS and IMU data are conducted. Then, an RSS propagation em-

pirical formula is given to obtain a higher positioning accuracy. A hybrid positioning algorithm is proposed based on the adaptive Kalman filter (AKF) and weighted least squares (WLS) trilateration which fuses the VLC RSS and IMU data together to calculate the positioning solution. The hybrid positioning algorithm is evaluated by using the developed platform with the experimental results.

1 System Description

The IPS shown in Fig. 1 consists of three main parts: the LED-based transmitter, receiver and positioning server. The receiver is equipped with an advanced RISC machine (ARM), which collects measurement data and transmits the information to the server. Then, the positioning server applies the hybrid positioning algorithm to estimate and display the positioning results.
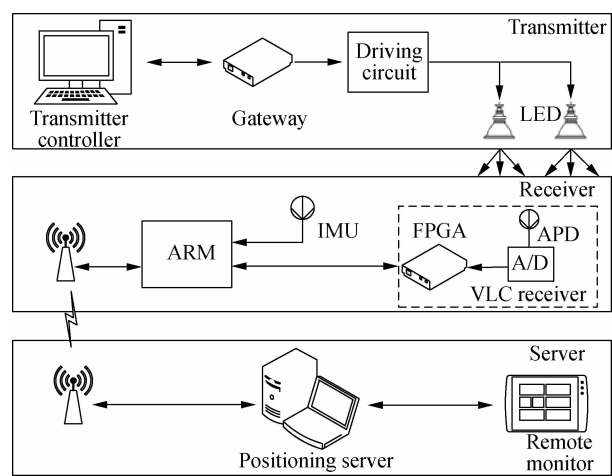

Fig. 1 System architecture of the indoor positioning system

1.1 LED-based transmitter and protocol design

The transmitter consists of the controller, gateway and LED transmitter. The controller serves to control and set the parameters of gateway. The gateway is a programmed device of the field programmable gate array (FPGA). It executes controlling instructions and transmits the message to LEDs or to another gateway. The LED transmitter includes the driving circuit and LED. When the gateway receives the controlling commands, it can change its configurations or activate its transmitters.

To ensure a good performance of the VLC system, the on-off keying (OOK) modulation is used at the transmitter due to its low complexity and high transmission rate. The signal is encoded into "0" or "1" by Manchester encoding. All the LEDs transmit their own ID data during their own time slot. The frame structure includes the header, unique identification (UID) of the transmitter, data and tail.

1.2 ARM-based receiver

There are three main parts: the IMU, VLC receiver and ARM in the receiver, as shown in Fig. 2. ARM is not only used for data transformation, but also works as a controller and gateway. The VLC RSS and IMU data will be collected by ARM with timestamps, and then ARM sends the data to the next gateway or server. ARM can change the configurations and transmit the feedback message to the server.

IMU consists of a three-axis accelerometer and a three-axis gyroscope (magnetometer sensors are often unreliable), which has been generally aligned during manufacturing and placed horizontally on the mobile target. The coordinate system on the grid body of IMU is assigned to be the body frame, and the inertial navigation coordinate system is assigned to be the global frame correspondingly. The VLC receiver with avalanche photodiode (APD) and analog-to-digital (AD) converts the optical signal into an electrical signal and then obtains the RSS and the ID data. The RSS measurement and the corresponding ID will be put into a fixed-length frame and then sent to ARM by FPGA.

1.3 Positioning server

The hybrid positioning algorithm is applied in the server, which is composed of three modules. The network control module plays a significant role in improving the performance of communication and positioning. In this
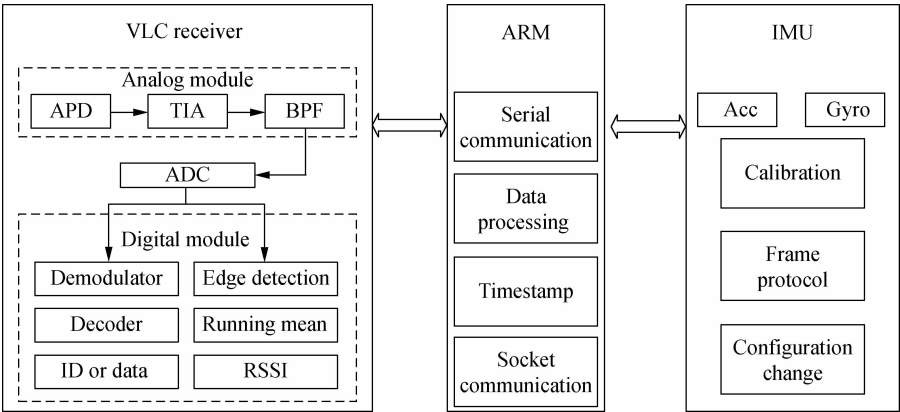

Fig. 2 Framework of the ARM-based receiver

paper, only one receiver is considered, so the details of this function will not be discussed here. The data storage and processing module reads the raw data package, and it saves the necessary data and final positioning solutions into the database. After the position solution is obtained, the module can send the real-time position to the display module.

2 Measurement Preprocessing

In this section, the measurement calibration is described in detail. The bias and drifts of calibration formula will be updated to improve the accuracy of the measured data. Then, a propagation empirical formula is proposed to calculate the distances from reference points to the mobile target based on RSS.

2.1 Measurement calibration

With the measured acceleration $\tilde{a}$ and angular velocity $\tilde{\omega}$ of the mobile target, the acceleration and angular velocity after calibration[13] are shown as

$$a = C_g^b \tilde{a} + b_{ac} + n_{ac} \tag{1}$$

$$\omega = C_g^b \tilde{\omega} + b_{av} + n_{av} \tag{2}$$

where b_{ac} is the acceleration bias; b_{av} is the angular velocity drift; and C_g^b is the rotation matrix that can transform the measurement data from the global frame to the body frame based on quaternion[14]. The process and measurements are modeled as linear Gaussian. The noise n_{ac} and n_{av} are i. i. d Gaussian sequences with variance σ_{ac}^2 and σ_{av}^2, respectively.

In this system, the RSS is denoted as the received power of the electrical signal. Before the distance calculation, the calibration procedure is required. A set of $RSS = \{RSS_1, \ldots, RSS_i, \ldots, RSS_C\}$ are collected with known horizontal distances $r = \{r_1, \ldots, r_i, \ldots, r_C\}$. C is the number of the measured RSS. The calibration formula of RSS_i is given as

$$u_i = U(RSS_i) = G (RSS_i + b_j) + n_j \tag{3}$$

where G is the gain; b_j is the bias; n_j is the noise, which is assumed to be additive Gaussian noise with covariance σ_j^2. As time progresses, the errors of RSS measurements will be affected by the resistance temperature coefficient. During positioning, the gain and bias will be updated based on the RSS propagation model.

2.2 RSS propagation model

According to the Lambertian law[15], the receive power of the electrical signal is calculated considering the irradiance angle, the effective area of the receiver photodiode, the filter gain and concentrator gain. The Lambertian law requires that the medium must be homogeneous and the incident radiation must be strictly parallel, which are difficult to fulfill in a practical environment. However, there is a snoot attached to the LED to increase the effective luminous intensity[16]. Therefore, the real indoor positioning system cannot meet the strict environment requirements of Lambertian law.

To obtain a more accurate horizontal distance from the receiver to LEDs, a novel empirical formula is given with the data RSS and horizontal distance r. With the vertical receiver and horizontal transmitter, the measurements of VLC RSS and horizontal distance are collected to fit the empirical formula. The height of LEDs is 2.25 m, and the horizontal distance r_i is calculated by the empirical formula $R(u_i)$ with normalized RSS u_i from Eq. (3) which is shown as

$$r_i = R(u_i) = p_0 + p_1 u_i + p_2 u_i^2 + p_3 u_i^3 + p_4 u_i^4 \tag{4}$$

where $p_0 = 58$, $p_1 = -76$, $p_2 = -11$, $p_3 = 116$, and $p_4 = -84$. The fitting precision is high and the empirical formula is reliable in this IPS. Finally, the comparison between the empirical formula and Lambertian law is shown in Fig. 3. It is clear that the empirical formula is closer to the real data than the traditional model.
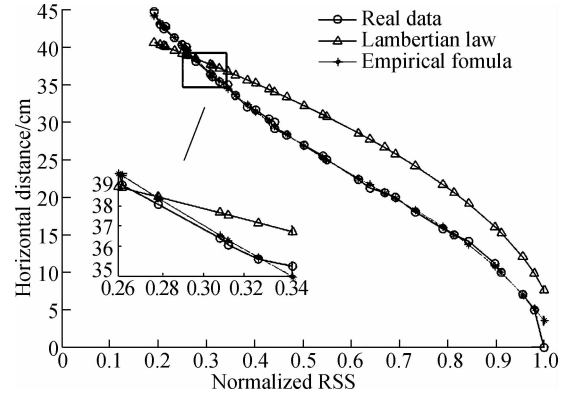

Fig. 3 Comparison between empirical formula and Lambertian law

The normalization is required during positioning, and G and b_j in Eq. (3) are shown as

$$G = \frac{1}{\max(RSS_i)} \tag{5}$$

$$b_j = \arg\min_{(b_j)} \sum_{i=1}^{N} | r_i - R(U(RSS_i)_0) |^2 \tag{6}$$

where $U(RSS_i)_0 = U(RSS_i \mid b_j = 0)$ and $R(\cdot)$ is the RSS propagation function the same as that in Eq. (4).

Before positioning, the calibration parameters b_{ac}, b_{av}, G and b_j can be calculated to calibrate the measurements before the hybrid positioning algorithm is used. During positioning, the calibration parameters are updated by Eq. (5) and Eq. (6).

3 Hybrid Positioning Algorithm

The receiver placed on the mobile target is required to start under the illumination range of VLC to obtain an initial position. First, the measurements of acceleration,

angular velocity and RSS are calibrated. Then, the distance from the receiver to the LED can be calculated by the empirical formula, and the coordinate of the mobile target can be given by the proposed algorithm.

3.1 AKF with dynamic model

Since the calculation of velocity v_k and yaw angle α_k of the mobile target are modeled by linear Gaussian noise, the Kalman filter is adopted to obtain a higher accuracy with a lower computational complexity. The prediction process and measuring process are represented as

$$x_k = Ax_{k-1} + W_k \tag{7}$$

$$z_k = Hx_k + N_k \tag{8}$$

where k is the discrete-time tracking filter's time-index for positioning, and the state vector x_k and the measurement vector z_k are defined as

$$x_k = [\begin{array}{cccc} v_k & \alpha_k & \ddot{a}_k & \ddot{\omega}_k \end{array}]^T, \quad z_k = [\begin{array}{cc} \ddot{a}_{z,k} & \ddot{\omega}_{z,k} \end{array}]^T \tag{9}$$

where $\ddot{a}_k$ and $\ddot{\omega}_k$ are the predictive values of acceleration and angular velocity, respectively; $\ddot{a}_{z,k}$ and $\ddot{\omega}_{z,k}$ are the measurements of acceleration and angular velocity, respectively.

After calibration, acceleration and angular velocity can be obtained as $a = [\begin{array}{ccc} a_x & a_y & a_z \end{array}]^T$ and $\omega = [\begin{array}{ccc} \omega_\alpha & \omega_\beta & \omega_\gamma \end{array}]^T$, where α, β and γ are Euler angles. The yaw angle α is the moving direction, and v_k and α_k of the mobile target can be calculated by

$$v_k = v_{k-1} + \frac{\dot{a}_{k-1} + \dot{a}_k}{2} T + n_{v,k} \tag{10}$$

$$\alpha_k = \alpha_{k-1} + \frac{\dot{\omega}_{k-1} + \dot{\omega}_k}{2} T + n_{\alpha,k} \tag{11}$$

where $\dot{a}_k = \parallel a_{x,k} + a_{y,k} + a_{z,k} \parallel$; $\dot{\omega}_k = \omega_\alpha$; $\ddot{\omega}_{z,k} = (\dot{\omega}_{k-1} + \dot{\omega}_k)/2$; and T denotes the update interval. The noise of v_k and α_k are i.i.d Gaussian sequences with variance σ_v^2 and σ_α^2. The state matrix A and observed matrix H are given as

$$A = \begin{bmatrix} 1 & 0 & T & 0 \\ 0 & 1 & 0 & T \\ 0 & 0 & 1 & 0 \\ 0 & 0 & 0 & 1 \end{bmatrix}, \quad H = \begin{bmatrix} 0 & 0 & 1 & 0 \\ 0 & 0 & 0 & 1 \end{bmatrix} \tag{12}$$

W_k and N_k[17] are the noise vectors in the prediction process and observed process, which are presented as

$$W_k = [\begin{array}{cccc} w_{v,k} & w_{\alpha,k} & w_{ac,k} & w_{av,k} \end{array}]^T, \quad N_k = [\begin{array}{cc} n_{ac,k} & n_{av,k} \end{array}]^T \tag{13}$$

Theoretically, noise $w_{v,k}$ and $w_{\alpha,k}$ are equal to $n_{v,k}$ and $n_{\alpha,k}$; and $w_{ac,k}$, $w_{av,k}$, $n_{ac,k}$ and $n_{av,k}$ are i.i.d Gaussian sequences with variance σ_{ac}^2 and σ_{av}^2, respectively. However, in practice, the process noise covariance matrix

and the measurement noise covariance matrix are time-varying so that the tracking will be diverging[18]. Therefore, the AKF with a fault-tolerant memory attenuation is adopted to ensure the robustness when the covariance matrix is not positive[19]. Q_k and R_k denote the covariance matrices of W_k and N_k, which are shown as

$$Q_{k+1} = (1 - \zeta_k) Q_k + \zeta_k [\, \text{diag}(\tau_k) \,]$$

$$R_{k+1} = (1 - \zeta_k) R_k + \zeta_k [\, \text{diag}(K_k \tau_k K_k^T) \,] \tag{14}$$

where $\zeta_k = (1 - p)/(1 - p^{k+1})$ is the amnestic factor; p is a forgetting factor in the range from 0.95 to 0.995[18]; $\tau_k = (z_k - z_{k|k+1})(z_k - z_{k|k+1})^T$ is the residual between the measurement and prediction.

3.2 WLS for trilateration

The illustration of the algorithm based on trilateration is shown in Fig. 4. Suppose that the corresponding horizontal coordinate $(X^{(i)}, Y^{(i)})$ of LED i is known, and the horizontal distance r_i from the receiver to LED i can be calculated by Eq. (7). l_k is the displacement calculated by IMU data, $l_k = v_k T$. When more than one RSS measurement is collected, the coordinate of mobile target (x_k, y_k) can be calculated as

$$\left. \begin{array}{l} (x_k - X^{(1)})^2 + (y_k - Y^{(1)})^2 = r_{1,k}^2 \\ \vdots \\ (x_k - X^{(i)})^2 + (y_k - Y^{(i)})^2 = r_{i,k}^2 \\ \vdots \\ (x_k - X^{(m)})^2 + (y_k - Y^{(m)})^2 = r_{m,k}^2 \\ (x_k - x_{k-1})^2 + (y_k - y_{k-1})^2 = l_k^2 \end{array} \right\} \tag{15}$$

Assume that the measurements are influenced by an i.i.d Gaussian random variable with zero mean, the method of ordinary least squares (OLS) used for coordinates $S_k = [\begin{array}{cc} x_k & y_k \end{array}]^T$ is adopted as

$$A_{LS} S = b_{LS} \tag{16}$$

where

$$A_{LS} = \begin{bmatrix} 2(X^{(1)} - x_{k-1}) & 2(Y^{(1)} - y_{k-1}) \\ 2(X^{(2)} - x_{k-1}) & 2(Y^{(2)} - y_{k-1}) \\ \vdots & \vdots \\ 2(X^{(m)} - x_{k-1}) & 2(Y^{(m)} - y_{k-1}) \end{bmatrix}$$

$$b_{LS} = \begin{bmatrix} X^{(1)2} + Y^{(1)2} - r_{1,k}^2 - (x_{k-1}^2 + y_{k-1}^2 - l_k^2) \\ X^{(2)2} + Y^{(2)2} - r_{2,k}^2 - (x_{k-1}^2 + y_{k-1}^2 - l_k^2) \\ \vdots \\ X^{(m)2} + Y^{(m)2} - r_{m,k}^2 - (x_{k-1}^2 + y_{k-1}^2 - l_k^2) \end{bmatrix}$$

To improve the accuracy of coordinate S_k in estimation, LS is weighted based on the distances and weight W_{LS} is presented as

$$W_{\mathrm{LS}} = \begin{bmatrix} 1 - \dfrac{l_k}{\sum\limits_{i=1}^{m} r_{i,k} + l_k} \\[2ex] 1 - \dfrac{r_{1,k}}{\sum\limits_{i=1}^{m} r_{i,k} + l_k} \\[2ex] \vdots \\[1ex] 1 - \dfrac{r_{m,k}}{\sum\limits_{i=1}^{m} r_{i,k} + l_k} \end{bmatrix} \qquad (17)$$

Therefore, the coordinate S_k with the minimum mean squared error of b_{LS} and $A_{\mathrm{LS}} S_k$ in WLS is described as

$$[x_k \quad y_k]^{\mathrm{T}} = \arg\min_{(x,y)} [\,(b_{\mathrm{LS}} - A_{\mathrm{LS}} S_k)^{\mathrm{T}} W_{\mathrm{LS}} (b_{\mathrm{LS}} - A_{\mathrm{LS}} S_k)\,]$$

$$(18)$$

However, in the actual positioning environment, the light from the LED is sheltered or dissipated and the positioning area is limited by the illumination area. As shown in Fig. 4, there are three cases when taking the situation that the receiver receives different numbers of RSS measurements into consideration.

Case 1   When multiple RSS measurements are collected, the calculation is demonstrated as Eqs. (14) to (17).

Case 2   When only one RSS measurement is collected, the position of mobile target S_k can be calculated by

$$\left. \begin{array}{l} \dfrac{y_k - y_{k-1}}{x_k - x_{k-1}} = \tan \alpha_{k-1} \\[1ex] (x_k - x_{k-1})^2 + (y_k - y_{k-1})^2 = l_k^2 \\[1ex] (x_k - X^{(i)})^2 + (y_k - Y^{(i)})^2 = r_{i,k}^2 \end{array} \right\} \qquad (19)$$

Case 3   When no RSS measurement is collected, if the initial coordinate is given from the VLC positioning solution, the coordinate of mobile target S_k can be calculated by

$$\left. \begin{array}{l} x_k = x_{k-1} + l_k \cos \alpha_{k-1} \\ y_k = y_{k-1} + l_k \sin \alpha_{k-1} \end{array} \right\} \qquad (20)$$

where α_{k-1} is the yaw angle at time $k-1$. Due to the drifts, the error of results from IMU positioning will increase over time and the initial coordinate is required.

Take four LEDs as an example in Fig. 4. Using the triangulation positioning algorithm to calculate the coordinate in Case 1 needs no less than three reliable RSS measurements. Therefore, the available VLC positioning area only includes area 3 and area 4. With the IMU data, the position can be calculated when receiving less than three RSS measurements or even when the mobile target is away from the illumination area. The hybrid positioning algorithm is described in Algorithm 1.

Algorithm 1   AKF-WLS algorithm for data fusion indoor positioning

Input: $\tilde{a}$, $\tilde{\omega}$, $\{(X^{(1)}, Y^{(1)}), ..., (X^{(M)}, Y^{(M)})\}$, $\{\mathrm{RSS}_1,$
..., $\mathrm{RSS}_i, ..., \mathrm{RSS}_C\}$, $\{r_1, ..., r_i, ..., r_C\}$, $\tilde{a}_k$, ω_k, $\{\mathrm{RSS}_1,$
..., $\mathrm{RSS}_m\}_k$.

Output: Position estimation (x_k, y_k).

    Initialize G via Eq. (4), b_{ac}, b_{av} and $b_j = 0$.

    Obtain the fitting function as $R(u)$, update b_j via Eq. (5).

    Calculate $U(\mathrm{RSS}_i)$, a_k and ω_k by the calibration of $\tilde{a}_k$, $\tilde{\omega}_k$, $\mathrm{RSS}_{i,k}$ via Eqs. (1) to (3).

    for $i = 1, 2, ..., k$ do

      Update b_{ac}, b_{av}, G and b_j

    end for

    Calculate v_k and α_k by the AKF via Eqs. (3) to (14)

    if $\{\mathrm{RSS}_1, ..., \mathrm{RSS}_m\}_k \neq \varnothing$ then

      Calculate $r_{i,k}$ via Eq. (6)

      if size $\{\mathrm{RSS}_1, ..., \mathrm{RSS}_m\}_k > 1$ then

        Update weight W_{LS} via Eq. (17)

        Calculate position by the WLS via Eqs. (15) and (16)

        Obtain optimal position via Eq. (18)

      else

        Calculate position via Eq. (19)

      end if

    else
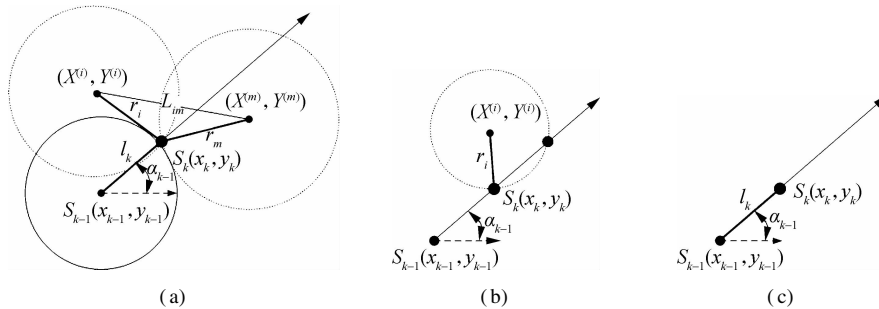
      Calculate position via Eq. (20)

    end if

Fig. 4   Illustration of the hybrid positioning algorithm of three cases. (a) Case 1; (b) Case 2; (c) Case 3

4   Experimental Results

In this section, the experiments are set up to evaluate the proposed IPS and hybrid positioning algorithm. The localization scenario is a space of 1.5 m × 3 m and the vertical height is 2.25 m. The mobile target is a crawler

car which moves horizontally with a velocity of 0.4 m/s. To achieve the initial position, the mobile target is required to start in the effective range of VLC positioning. There are nine LEDs as shown in Fig. 5. The gravity is 9.791 883 m/s², and the latitude is 31.220 2 rad.
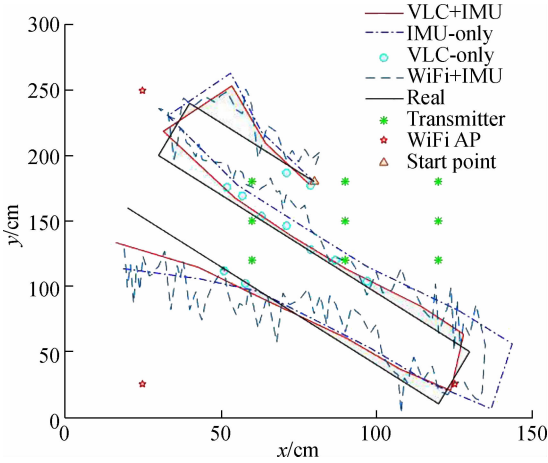

Fig. 5 Position solutions of different algorithms and real position

Fig. 5 illustrates the positioning results of the proposed hybrid positioning algorithm in this IPS with the algorithms using IMU-only, VLC-only and tightly-coupled integration of WiFi and MEMS sensors[20]. The irradiation diameter of each LED is about 0.8 m. The area that receives more than two RSS measurements is 44% of the illumination area, which means that the available range of the proposed hybrid positioning algorithm is two times that of the VLC-only algorithm. The mobile target moves from coordinate (80 cm, 280 cm) and stops at coordinate (20 cm, 260 cm). Since the initial position of IMU-only is given from a real position, the results from IMU-only are close to the real position at the beginning. Comparing the position solutions from the proposed hybrid positioning algorithm with the solutions from IMU-only algorithm, the position errors of IMU-only increase steadily. Only when the mobile target is in the LED illumination area, can the VLC-only algorithm provide positioning solutions with a high precision. The figure also shows that the solutions from integration of WiFi and the IMU algorithm lack smoothness with low accuracy.

The curves in Fig. 6 represent the cumulative distribution function (CDF) of position errors when the mobile
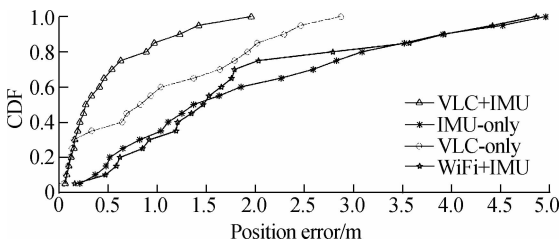

Fig. 6 Cumulative distribution function of position errors

target has moved approximately 50 m. The experimental results show that the CDF of VLC-only is similar to that of the proposed hybrid positioning algorithm, but the VLC-only algorithm can provide good results only when the mobile target moves under the illumination area. As time progresses, the maximum error of the IMU-only algorithm increases to about 5 m. The maximum error of the proposed hybrid positioning algorithm is less than 2 m, which is better than that from the integration of WiFi and the IMU algorithm with the maximum error of 4.86 m. The results of the proposed hybrid positioning algorithm show that it has calibrated the cumulative errors of IMU measurement and improves the positioning accuracy.
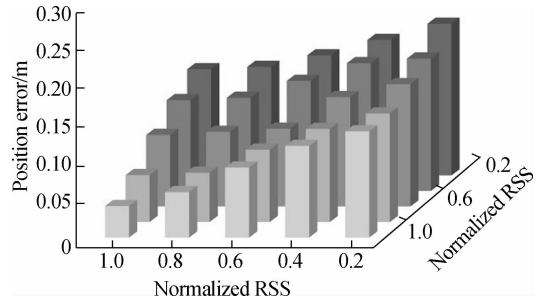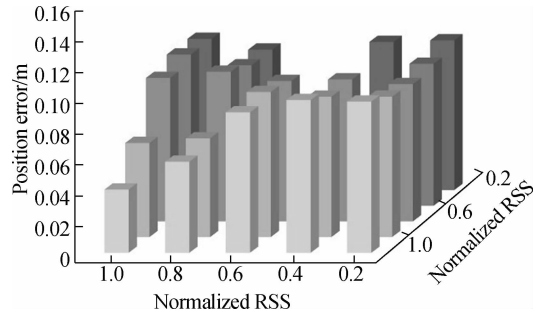
Fig. 7 Relationship between average position errors and normalized RSS. (a) VLC-only; (b) VLC + IMU

Fig. 7 shows the relationship between average position errors and normalized RSS. The average position errors from the proposed hybrid positioning algorithm and VLC-only algorithm are compared. When the mobile target moves with high normalized RSS, the position results from the proposed hybrid positioning algorithm are similar to those of the VLC-only algorithm. As the normalized RSS drops, the position errors of the VLC-only algorithm increase, but the position errors of the proposed hybrid positioning algorithm can be limited within 0.1 m. In Fig. 8, the distributions of localization errors from the proposed hybrid positioning algorithm and IMU-only algorithm are investigated when the mobile target moves 1 lap and 10 laps. The figure shows that 90% of position errors of the proposed hybrid positioning algorithm are no more than 0.2 m. Only if the mobile target is away from the illumination range for a long time,
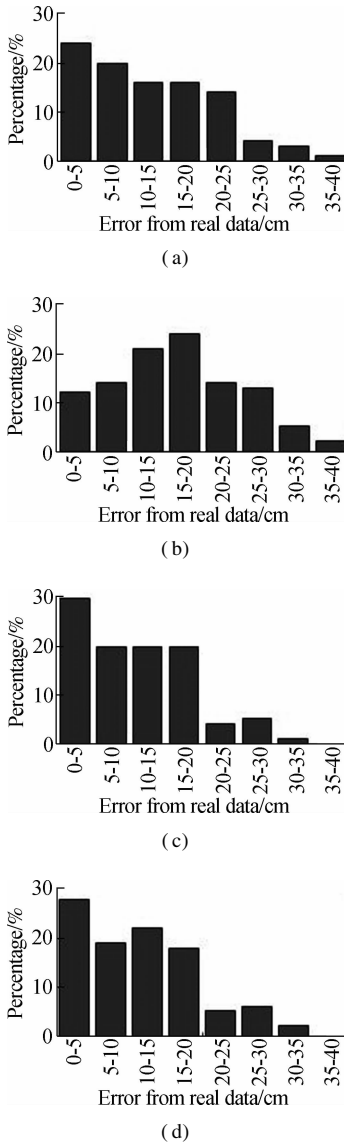
Fig. 8 Position errors range distribution of 1 lap and 10 laps. (a) The IMU position error of 1 lap; (b) The IMU position error of 10 lap; (c) The AKF-WLS position error of 1 lap; (d) The AKF-WLS position error of 10 laps
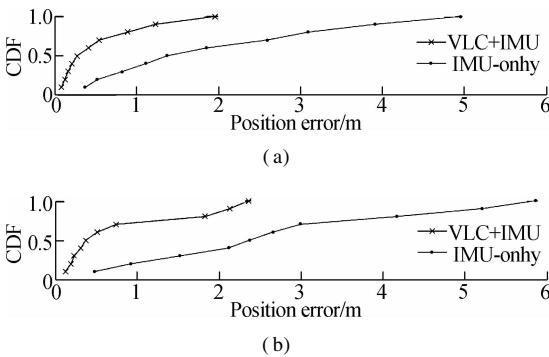

Fig. 9 Position errors cumulative distribution function with different velocities. (a) With velocity of 0.4 m/s; (b) With velocity of 0.8 m/s

will the errors increase larger than 0.25 m. The average error of the proposed algorithm is 86% that of the IMU-only algorithm average error. Due to the cumulative er-

rors, when the mobile target moves 10 laps, the average error of the IMU-only algorithm increases to be around two times that of the average error of 1 lap. At the same time, the proposed hybrid positioning algorithm can limit an average error under 0.15 m after 10 laps, which is 60% that of the IMU-only algorithm. The CDF in Fig. 9 shows that the increase of velocity will affect the performance of positioning. When the mobile target has moved approximately 50 m, the maximum error of the proposed algorithm is about 3 m lower than that of the IMU-only algorithm with the velocity of 0.4 m/s and the gap is up to about 3.5 m with the velocity of 0.8 m/s. As shown in the figure, the comparison between the proposed hybrid positioning algorithm and IMU-only algorithm illustrates that the proposed algorithm provides a much more precise positioning accuracy than the IMU-only with higher velocity. Therefore, the IPS based on the proposed hybrid positioning algorithm can not only extend the VLC localization range, but also calibrate the positioning of the IMU.

5 Conclusion

An indoor positioning system is designed by applying a hybrid positioning algorithm which fuses the VLC RSS and IMU data for mobile target tracking. The alignment before localization can reduce the measurement errors of IMU and VLC RSS. Experimental results show that the developed IPS using the proposed hybrid positioning algorithm can extend the positioning range of VLC positioning, mitigate the drifts of IMU data and reduce the positioning error. The developed IPS using the proposed hybrid positioning algorithm has been demonstrated to be a very competitive method for indoor positioning, which can provide a promising approach for indoor positioning research.

References

[1] He K, Zhang Y, Zhu Y, et al. A hybrid indoor positioning system based on UWB and inertial navigation [C]// *IEEE International Conference on Wireless Communications & Signal Processing*. Hefei, China, 2015: 1 − 5.

[2] van M T, van Tuan N, Son T T, et al. Weighted k-nearest neighbour model for indoor VLC positioning[J]. *IET Communications*, 2017, **11**(6): 864 − 871. DOI: 10. 1049/iet-com. 2016. 0961.

[3] Nakazawa Y, Makino H, Nishimori K, et al. LED-tracking and ID-estimation for indoor positioning using visible light communication [C]// *IEEE International Conference on Indoor Positioning and Indoor Navigation*. Busan, South Korea, 2015: 87 − 94.

[4] Wu C S, Yang Z, Liu Y H. Smartphones based crowdsourcing for indoor localization[J]. *IEEE Transactions on Mobile Computing*, 2015, **14**(2): 444 − 457. DOI: 10. 1109/tmc. 2014. 2320254.

[5] Li Q L, Wang J Y, Huang T, et al. Three-dimensional indoor visible light positioning system with a single trans-

mitter and a single tilted receiver[J]. *Optical Engineering,* 2016, **55**(10): 106103. DOI: 10. 1117/1. oe. 55. 10. 106103.

[6] Aghili F, Su C Y. Robust relative navigation by integration of ICP and adaptive Kalman filter using laser scanner and IMU [J]. *ASME Transactions on Mechatronics*, 2016, **21**(4): 2015 − 2026. DOI: 10. 1109/tmech. 2016. 2547905.

[7] Won S H P, Melek W W, Golnaraghi F. A Kalman/particle filter-based position and orientation estimation method using a position sensor/inertial measurement unit hybrid system[J]. *IEEE Transactions on Industrial Electronics*, 2010, **57**(5): 1787 − 1798. DOI: 10. 1109/tie. 2009. 2032431.

[8] Lü H, Feng L H, Yang A Y, et al. High accuracy VLC indoor positioning system with differential detection[J]. *IEEE Photonics Journal*, 2017, **9**(3): 1 − 13. DOI: 10. 1109/jphot. 2017. 2698240.

[9] Krommenacker N, Vásquez O C, Alfaro M D, et al. A self-adaptive cell-ID positioning system based on visible light communications in underground mines [C]// 2016 *IEEE International Conference on Automatica*. Curico, Chile, 2016: 16525691. DOI: 10. 1109/ICA-ACCA. 2016. 7778427.

[10] Guan W P, Wu Y X, Wen S S, et al. A novel three-dimensional indoor positioning algorithm design based on visible light communication [J]. *Optics Communications*, 2017, **392**: 282 − 293.

[11] Jimenez Ruiz A R, Seco Granja F, Prieto Honorato J C, et al. Accurate pedestrian indoor navigation by tightly coupling foot-mounted IMU and RFID measurements[J]. *IEEE Transactions on Instrumentation and Measurement*, 2012, **61** (1): 178 − 189. DOI: 10. 1109/tim. 2011. 2159317.

[12] Liu W L. LiDAR-IMU time delay calibration based on iterative closest point and iterated sigma point Kalman filter [J]. *Sensors*, 2017, **17** (3): 539. DOI: 10. 3390/s17030539.

[13] Kumar G A, Patil A K, Patil R, et al. A LiDAR and IMU integrated indoor navigation system for UAVs and its application in real-time pipeline classification[J]. *Sensors*, 2017, **17**(6): 1268. DOI: 10. 3390/s17061268.

[14] Zhao Y W. Performance evaluation of cubature Kalman filter in a GPS/IMU tightly-coupled navigation system [J]. *Signal Processing*, 2016, **119**: 67 − 79. DOI: 10. 1016/j. sigpro. 2015. 07. 014.

[15] Zhang X L, Duan J Y, Fu Y G, et al. Theoretical accuracy analysis of indoor visible light communication positioning system based on received signal strength indicator [J]. *Journal of Lightwave Technology*, 2014, **32**(21): 4180 − 4186. DOI: 10. 1109/jlt. 2014. 2349530.

[16] Komine T, Nakagawa M. Fundamental analysis for visible-light communication system using LED lights [J]. *IEEE Transactions on Consumer Electronics*, 2004, **50** (1): 100 − 107. DOI: 10. 1109/tce. 2004. 1277847.

[17] Nguyen N T, Nguyen N H, Nguyen V H, et al. Improvement of the VLC localization method using the extended Kalman filter [C]// 2014 *IEEE Region* 10 *Conference*. Bangkok, Thailand, 2014: 14885864. DOI: 10. 1109/TENCON. 2014. 7022416.

[18] Fang X M, Nan L, Jiang Z H, et al. Robust node position estimation algorithms for wireless sensor networks based on improved adaptive Kalman filters[J]. *Computer Communications*, 2017, **101**: 69 − 81. DOI: 10. 1016/j. comcom. 2016. 11. 005.

[19] González R, Giribet J I, Patiño H D. An approach to benchmarking of loosely coupled low-cost navigation systems[J]. *Mathematical and Computer Modelling of Dynamical Systems*, 2014, **21** (3): 272 − 287. DOI: 10. 1080/13873954. 2014. 952642.

[20] Zhuang Y, El-Sheimy N. Tightly-coupled integration of WiFi and MEMS sensors on handheld devices for indoor pedestrian navigation[J]. *IEEE Sensors Journal*, 2016, **16**(1): 224 − 234. DOI: 10. 1109/jsen. 2015. 2477444.

基于 VLC 与 IMU 融合的移动物体跟踪室内定位系统

邹　倩　　夏玮玮　　张　静　　黄博南　　燕　锋　　沈连丰

(东南大学移动通信国家重点实验室,南京 210096)

摘要:利用可见光通信(VLC)和惯性测量单元(IMU),设计了室内定位系统(IPS),实现对移动物体的定位和跟踪. 该 IPS 平台包括发光二极管发射器、接收器和定位服务器 3 部分. 为了减少由测量引起的误差,提出了惯性传感数据校准模型和可见光通信 RSS 数据归一化校准模型对数据进行校准. 然后,通过建立的实际传播模型,从 RSS 数据中计算发射器和接收器之间的距离. 此外,提出了一种混合定位算法,使用自适应卡尔曼滤波器和加权最小二乘三边测量来估计移动物体的位置. 实验结果表明,采用所提混合定位算法的 IPS 能够扩展 VLC 的定位区域,减轻 IMU 漂移,提高移动物体的定位精度.

关键词:室内定位系统;可见光通信;惯性测量单元;混合定位算法

中图分类号:TN929. 5